THE JOURNAL OF BIOLOGICAL CHEMISTRY VOL. 281, NO. 15, pp. 10399–10409, April 14, 2006

Domain Analysis of a Groundnut Calcium-dependent Protein Kinase

*NUCLEAR LOCALIZATION SEQUENCE IN THE JUNCTION DOMAIN IS COUPLED WITH NONCONSENSUS CALCIUM BINDING DOMAINS**

Received for publication, October 7, 2005, and in revised form, January 12, 2006 Published, JBC Papers in Press, February 7, 2006, DOI 10.1074/jbc.M511001200

Ayan Raichaudhuri[‡1], Rajasri Bhattacharyya[§2], Shubho Chaudhuri[‡3], Pinak Chakrabarti[§], and Maitrayee DasGupta[‡4]

From the [‡]Department of Biochemistry, Calcutta University, 35, Ballygunge Circular Road, Calcutta 700019 and the [§]Department of Biochemistry and Bioinformatics Centre, Bose Institute, P1/12 CIT Scheme VIIM, Calcutta 700054, India

The signature of calcium-dependent protein kinases (CDPKs) is a C-terminal calmodulin-like domain (CaMLD) with four consensus calcium-binding sites. A junction domain (JD) joins the kinase with CaMLD and interacts with them through its autoinhibitory and CaMLD binding subdomains, respectively. We noted several CDPKs additionally have a bipartite nuclear localization signal (NLS) sequence as a subdomain in their JD, and this feature is obligatorily coupled with the absence of consensus calcium-binding sites in their respective CaMLDs. These predicted features are substantiated by undertaking investigations on a CDPK (gi:67479988) isolated from cultured groundnut (*Arachis hypogea*) cells. This kinase can bind 3.1 mol of Ca^{2+} under saturating conditions with a considerably high K_d of 392 μM as compared with its canonical counterparts. CD spectroscopic analysis, however, indicates the intramolecular structural changes accompanied with calcium binding to be similar to canonical CDPKs. Attesting to the presence of NLS in the JD, the endogenous kinase is localized in the nucleus of osmotically stressed *Arachis* cells, and *in vitro* binding assays indicate the NLS in the JD to interact with nuclear transport factors of the importin family. Homology modeling also indicates the feasibility of interaction of importins with the NLS present in the JD of such CDPKs in their activated form. The possible significance of obligatory coupling between the presence of NLS in the junction domain and atypical calcium binding properties of these CDPKs is discussed in the light of the known mechanisms of activation of these kinases.

CDPKs[5] are unique transducers of calcium signaling in plants and protists that are absent in yeasts and animals (1–3). The core structure of CDPKs has an N-terminal catalytic domain, a C-terminal calmodulin-like regulatory domain (CaMLD), and a junction domain sandwiched between these two domains. As the catalytic domain of CDPKs is most closely related to calmodulin-dependent protein kinases (CaMK), CDPKs are believed to have arisen from a fusion event between a CaMK and a calmodulin (CaM) gene (1, 4). In consistency, the mechanism of activation of CDPKs is largely similar to CaMKs (5–9). In CaMKs, the autoinhibitory and calmodulin binding domain is located immediately C-terminal to the kinase domain, and the autoinhibition is released in the presence of calcium and exogenous CaM (10). In CDPKs, the junction domain following the kinase domain is shown to contain subdomains possessing autoinhibitory and CaMLD binding properties. The autoinhibition is relieved by a calcium-dependent intramolecular interaction between the CaMLD and its target in the junction domain (7).

The distinguishing feature in the intramolecular activation of CDPKs is the covalent linkage of the CaMLD with its target in the same polypeptide. This linkage has been nicknamed as "tether" region and has been shown to provide a "structural constraint" that is essential for complete activation of a CDPK (9). Any insertion in the tether results in almost complete disruption in calcium-dependent activation of a CDPK. Thus, in addition to interaction of the CaMLD with its target in the junction domain, intramolecular activation of CDPKs involves a conformational change of the holoenzyme mediated through the tether.

Genomic sequencing as well as several extensively expressed sequence tag projects indicate the presence of multigene families of CDPKs in various plants (2, 11). They are demonstrated to be involved in regulating ion transport and/or gene expression linked with various cellular processes like cytoskeleton dynamics, stress response, growth and development, and metabolism (3). Such response specificity of individual CDPKs is believed to be generated by their varying subcellular compartmentalizations, varying calcium and lipid sensitivities, and differences in substrate recognition (2). The multiple subcellular locations of CDPKs include the plasma membrane, endoplasmic reticulum membrane, endosperm storage vesicles, cytoskeletal system, mitochondria, nucleus, and peroxisomes (12–17).

Here we report the domain analysis of a group of CDPKs, which apart from having the signature features of these kinases also have a bipartite nuclear localization sequence (18–21) in their junction domain. Interestingly, sequence analysis of all CDPKs in the data base reveals that the presence of NLS in their junction domains is obligatorily coupled with the presence of nonconsensus calcium binding EF hand loops (22–26) in their respective CaMLDs. We substantiate these predictions with biophysical and biochemical experiments undertaken with an *Arachis* CDPK that possess these features. In the light of the known mechanism of regulation of CDPKs (5–9), we discuss the possible reasons for the essentiality of coupling between the presence of an NLS in the JD and the nonconsensus calcium-binding motifs in the CaMLD.

* This work was supported in part by the Council of Scientific and Industrial Research, Government of India, Grant 38(1041)/02/EMR-II, 2002–2003. The costs of publication of this article were defrayed in part by the payment of page charges. This article must therefore be hereby marked "*advertisement*" in accordance with 18 U.S.C. Section 1734 solely to indicate this fact.

[1] Recipient of Fellowship 2-48/2001(i)-EU-II from the University Grants Commission, Government of India.

[2] Supported by the Department of Biotechnology, Government of India.

[3] Present address: School of Molecular Biosciences, Washington State University, Pullman, WA 99164-4660.

[4] To whom correspondence should be addressed. Tel.: 91-33-24753680; Fax: 91-33-24764419; E-mail: maitrayee_d@hotmail.com.

[5] The abbreviations used are: CDPK, calcium-dependent protein kinase; CaMK, calcium/calmodulin-dependent protein kinase; CaM, calmodulin; GST, glutathione *S*-transferase; CaMLD, calmodulin-like domain; NLS, nuclear localization signal; DAPK, death-associated protein kinase; IPTG, isopropyl 1-thio-β-D-galactopyranoside; MES, 4-morpholineethanesulfonic acid; PMSF, phenylmethylsulfonyl fluoride; JD, junction domain; W7, *N*-(6-aminohexyl)-5-chloro-1-naphthalene sulfonamide.

EXPERIMENTAL PROCEDURES

Materials

TOPO TA cloning kit was obtained from Invitrogen; pQE expression vectors, nickel-agarose, and anti-RGS-His antibody were obtained from Qiagen (Germany). Enzymes, glutathione-Sepharose 4B, Tris, Hepes, glycerol, Triton X-100, β-mercaptoethanol, aprotinin, leupeptin, and IPTG were obtained from Amersham Biosciences. PMSF, benzamidine, *N*-(6-aminohexyl)-5-chloro-1-naphthalene sulfonamide (W7), anti-tubulin antibody, 1-naphthalene acetic acid, and benzylaminopurine were obtained from Sigma. Western blotting kit was obtained from Roche Applied Science. Oligonucleotides were obtained from IDT. All other reagents of analytical grade were obtained from SRL (India). $^{45}Ca^{2+}$ (185 MBq, specific activity 79.5 mCi/g) was obtained from BRIT, Government of India.

Methods

Cell Cultures and Stress Treatments—Initiation and maintenance of an auxin autotrophic cell suspension culture of *Arachis hypogea* are discussed in detail in Ref. 27. In brief, the culture is maintained in MS medium (aux^-cyt^+) containing 11.09 μmol liter^{-1} of benzylaminopurine, in a gyratory shaker at 100 rpm at 27 °C under a 16/8-h photoperiod at 40 μmol of photons·m^{-2}·s^{-1}. The cells are subcultured every 7 days by inoculating 3 ml of cells packed at 1 × *g* in 50 ml of medium. For osmotic stress, 2 ml of packed volume of cells collected from logarithmic growth phase were incubated in 10 ml of aux^-cyt^+ media containing 0.4 M sucrose for 4 days (27–29). For auxin treatment, the stressed *Arachis* cells were treated for 1 h with 13.5 μmol liter^{-1} of 1-naphthalene acetic acid.

Cloning, Expression, and Purification of Arachis CDPK and Other Recombinant Polypeptides—Total RNA was isolated from osmotically stressed *Arachis* cells using RNeasy Plant mini kit (Qiagen) following the manufacturer's instructions. mRNA was isolated from this total RNA preparation using the Oligotex mRNA kit (Qiagen). The isolated mRNA was subjected to RT reaction using cDNA synthesis module (Amersham Biosciences) with random hexanucleotide and anchored dT_{25} primers. The cDNA for a *Arachis* CDPK was PCR-amplified using primers 5′-GCTCTAGAGG(T/A/G)(C/A)G(A/T/G/C)GG(T/A/G)-GA(A/G)TTC/TGG-3′ and 5′-CCCAAGCTTATCATCGCCACA-AATTC-3′ that corresponded to the sense sequence of domain I of the catalytic domain and antisense sequence of the fourth calcium-binding site of the CaMLD, respectively. The amplified 1.3-kb fragment was cloned in the TOPO TA vector from Invitrogen. The sequence named AhCPK2 was submitted to GenBank™ (gi:67479988). For expression of *Arachis* CDPK with a N-terminal His_6 tag, it was PCR-amplified using 5′-GGGGTACCTATATCCTTGATAGAGAACTTGGGCGGG-GGGAGTTCGGG-3′ as forward and 5′-CCCAAGCTTTCTCCA-ATCTGTTCCTGTCTTCATCATCGCCACAAATTCTTC-3′ as reverse primers, respectively, and subcloned into the KpnI-HindIII sites in Qiagen expression vector pQE30. For expressing the JD-CaMLD polypeptide with an N-terminal His_6 tag, a BamHI-HindIII fragment encompassing Ile-252 to Met-431 from AhCPK2 was subcloned in Qiagen expression vector pQE32. For expressing the CaMLD polypeptide (Ala-289 to Met-431) with a His_6 tag, cloning was done in two steps. First, the CaMLD domain of AhCPK2 was PCR-amplified using 5′-GCTCTAGAGCTGATTTCTTGTCC-3′ and 5′-CCCAAGCTTA-TCATCGCCACAAATTC-3′ as forward and reverse primers, respectively, and subcloned into the XbaI-HindIII sites of pUC19. The BamHI-HindIII fragment from the pUC19 backbone was then cloned into the Qiagen expression vector pQE30. Mutations were introduced in the JD-CaMLD polypeptide by PCR using 5′-CGGGATCCCAAA-TGCTAGGAGTGGCTCCAAATATTCCTCTTGGGGATGCTG-TTCTATCAAGACTTAAG-3′ and 5′-CCCAAGCTTATCATCGC-CACAAATTC-3′ as the forward and the reverse primers, respectively. The amplified fragment was cloned into the BamHI-HindIII sites in Qiagen expression vector pQE30 for expressing the JD-$CaMLD_{mut}$. Nucleotide sequence and in-frame ligation was checked for all the clones by DNA sequencing. The recombinant polypeptides were expressed in *Escherichia coli* M15 by growing in the presence of 1 mM IPTG for 5 h at 37 °C, and the proteins were purified under nondenaturing conditions using nickel-nitrilotriacetic acid-agarose (Qiagen) at 4 °C by the procedures recommended by the manufacturers. The final preparation of the polypeptides were dialyzed against 20 mM Tris-HCl, pH 7.4, and stored in aliquots in −80 °C. The purified recombinant proteins were analyzed for purity and integrity by SDS-PAGE (30). The protein concentrations were determined using Bradford method (31).

The JD-CaMLD and the CaMLD polypeptides from *Arabidopsis* CDPK AtCPK1 (32) were expressed in *E. coli* BL21 grown in M9, glucose, 0.5% tryptone in the presence of 0.5 mM IPTG for 4–6 h at 25 °C, and the proteins were purified at 4 °C using nickel-nitrilotriacetic acid-agarose (Qiagen) beads according to the manufacturer's instruction.

The GST-importin fusion proteins (33) were expressed in *E. coli* BL21 in the presence of 0.5 mM IPTG for 4–6 h at 20 °C, and the proteins were purified at 4 °C using glutathione-Sepharose beads according to the manufacturer's instruction (Amersham Biosciences). 2 mM dithiothreitol was included in all the solutions throughout the purification procedures. The final preparation of the polypeptides were dialyzed against 20 mM Tris-HCl, pH 7.4, and stored in aliquots in −80 °C.

Bioinformatics—Sequences of *Arabidopsis* CDPK family members were retrieved from the PlantsP Data Base (plantsp.sdsc.edu). CDPK sequences containing NLS in their junction domain coupled with non-canonical EF hands in their calmodulin-like domains were identified by manually analyzing all entries in the GenBank™ (www.ncbi.nlm.nih.gov) or SwissProt database by using PROSITE (34). Sequences were aligned with ClustalW (35).

Ca^{2+} Binding to Proteins—The calcium binding property was measured by equilibrium dialysis as described previously (36). For ensuring a calcium-free condition, all buffers and protein solutions were passed through a Chelex 100 column (Bio-Rad). The plasticwares were soaked in 2.5 mM EDTA overnight, and dialysis bags were heated at 80 °C in 1 mM EDTA, 1 mM $NaHCO_3$ for 1 h, and both were rinsed with calcium-free water. 40 μl (10 μM) of the purified polypeptide was dialyzed for 24 h at 25 °C against 400 μl of a solution of 25 mM MES-KOH, pH 6.0, containing 150 mM KCl and $^{45}Ca^{2+}$ (0.25 μCi/ml) in presence of indicated concentrations of $CaCl_2$. After dialysis, 20 μl of the protein solution and the external solution were collected from each of the dialysis set ups. The collected solutions were spotted on nitrocellulose membrane (13 mm in diameter), and radioactivity associated was measured. The moles of bound calcium/mol of protein and the concentration of unbound calcium were evaluated from the known concentration of the protein and the initial calcium concentration. The calcium binding data were processed according to the Hill model (37, 38) using Kyplot. The Hill model provides information regarding the degree of cooperativity (Hill constant, *A*3), the maximum number of calcium-binding sites (*A*1), and apparent dissociation constant (*A*2) according to Equation 1,

$$y = \frac{A1}{\left(1 + \frac{A2}{x}\right)^{A3}} \qquad \text{(Eq. 1)}$$

where *y* and *x* denote the average number of moles of calcium bound/mol of protein and the free calcium concentration, respectively.

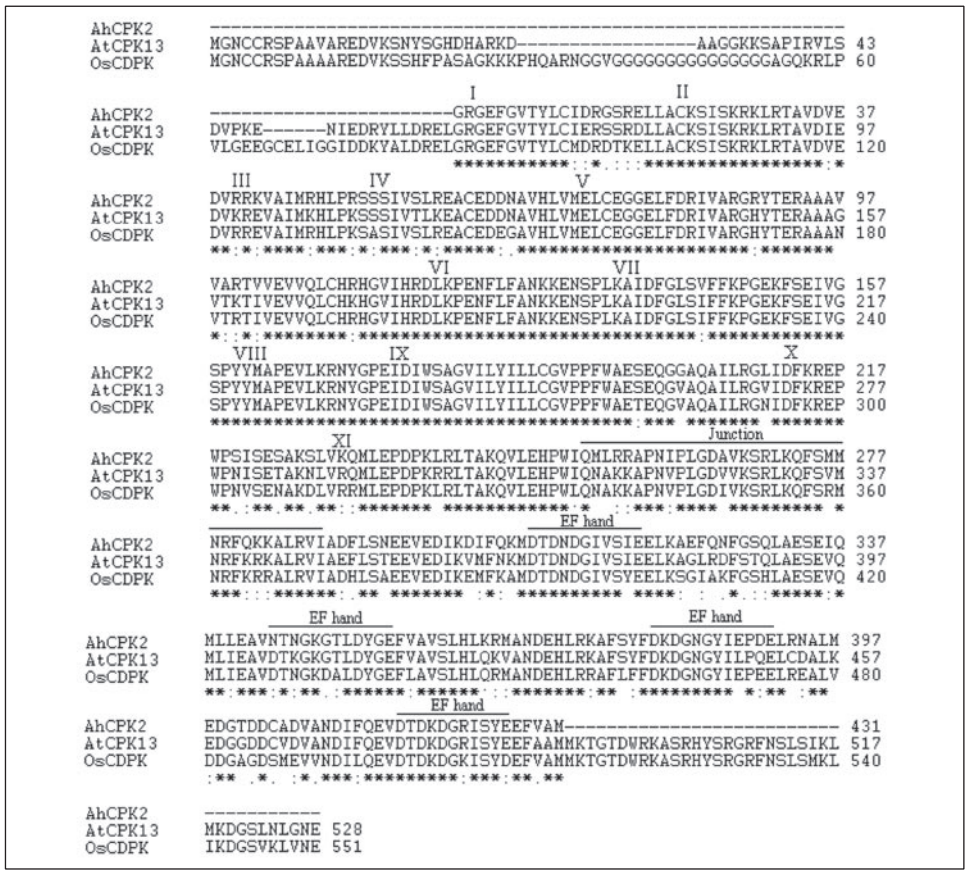

FIGURE 1. **Conserved domains in AhCPK2.** Alignment of *Arachis* CDPK AhCPK2 (gi:67479988) with *Arabidopsis* CDPK AtCPK13 (gi:28059078) and *Oryza* CDPK (gi:34907990) using ClustalW (multiple sequence alignment). Identical amino acids are indicated by *asterisks*, and similar amino acids are marked with *single dots* and *colons*. Catalytic domains (*I–IX*), Junction domain, and EF hands of CaMLD domain of AhCPK2 are marked.

Circular Dichroism—Experiments were performed on Jasco-720 spectropolarimeters. A bandwidth of 1 nm and a scan step size of 0.25 nm were employed with a 0.1-cm path length. Spectra were recorded at 298 K with 5 μM of the indicated polypeptides in 20 mM Tris-HCl, pH 7.4, in the presence of 1 mM calcium or 5 mM EGTA. Five scans were averaged for each sample, and the spectrum for the buffer was subtracted as a blank.

Cell Fractionation—Membrane fractions were isolated and purified from both normal and stressed *Arachis* cells with or without auxin treatment as described previously (28) and according to the procedures described in Refs. 12 and 39. In brief, cells were harvested, rinsed with distilled water, ground in a mortar cooled with liquid nitrogen, and extracted with ice-cold 50 mM Tris-HCl, pH 7.4, containing 2 mM β-mercaptoethanol, 10 mM EDTA, 2.5 mM EGTA, 300 mM sucrose, and protease inhibitors (0.5 mM PMSF, 1 mM benzamidine, 10 μg ml^{-1} leupeptin, and 10 μg ml^{-1} aprotinin). To remove cell debris, the slurry (1 ml of buffer per g wet tissue) was first passed through cheesecloth and then centrifuged for 15 min at 2,000 $\times$ *g* (twice). The supernatant was subjected to centrifugation at 100,000 $\times$ *g* for 1 h. The microsomal membrane pellet obtained at this step was resuspended in resuspension buffer (10 mM Tris-HCl, pH 7.4, 1 mM EDTA, 1 mM EGTA, and protease inhibitors (0.5 mM PMSF, 1 mM benzamidine, 10 μg ml^{-1} leupeptin and 10 μg ml^{-1} aprotinin)). Membrane and soluble protein fractions were stored at −80 °C.

Nuclear extracts were prepared from normal and stressed *Arachis* cells as described in detail previously (29). The final nuclear pellet was resuspended in 20 mM Tris-HCl, pH 7.4, 5 mM $MgCl_2$, 500 mM NaCl, 0.5 mM PMSF, 1 mM benzamidine, 10 μg ml^{-1} leupeptin, 10 μg ml^{-1} aprotinin, 10% Triton X-100 and stored at −80 °C in small aliquots. Protein concentration was estimated by Bradford method (31).

Immunological Techniques—Antibodies against JD-CaMLD polypeptide of AhCPK2 was raised in rabbits. The affinity-purified His_6-tagged JD-CaMLD polypeptide was subjected to SDS-PAGE. After mild staining of the gel, the appropriate band was excised, crushed, and used for immunization according to standard protocols (40).

Western blotting with anti-AhCPK2 and anti-ABI3 (29) was done at 1:1000 dilutions using a kit from Roche Applied Science. Western blotting with anti-His and anti-tubulin was done according to the manufacturer's instructions.

GST Pull-down Assay—Interactions of the JD-CaMLD, CaMLD, and JD-$CaMLD_{mut}$ polypeptides with the importins were investigated by this assay following the binding conditions described previously (33, 41) with some modifications. In brief, 300 pmol of polypeptides were incubated in a total reaction volume of 150 μl in the presence of 20 mM Hepes, pH 7.3, 110 mM potassium acetate, 2 mM magnesium acetate, 5 mM sodium acetate, and 250 mM sucrose with the indicated concentrations of calcium and EGTA. Binding was done for 4 h at 4 °C. Glutathione-Sepharose 4B beads were added, gently mixed for 1 h, and then washed three times (15 min each) with 1× Tris-buffered saline containing the indicated concentrations of calcium or EGTA. The reaction mixture was analyzed in 12% SDS-PAGE (30) and Western-blotted with anti-His or anti-AhCPK2 antibody.

Homology Modeling—The model of *Arachis* CDPK, AhCPK2, was developed in two steps using the comparative modeling module of MODELLER (42). The necessary sequence alignments were done using ClustalW (35) (Fig. 7).

In the first step the model for JD bound to the calcium-bound CaMLD was modeled. The templates used were the files with codes

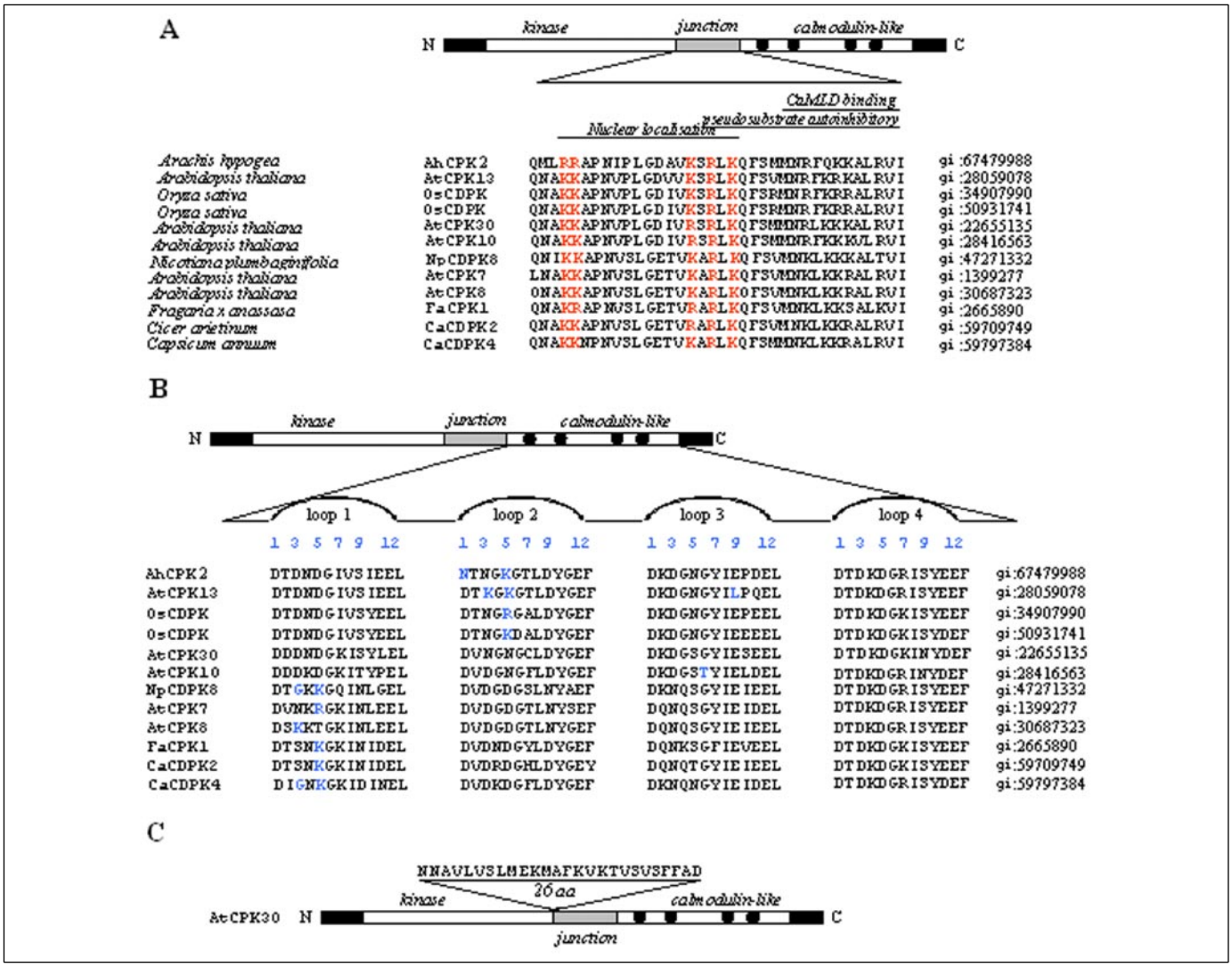

FIGURE 2. **Domain analysis of CDPKs containing an NLS in their junction domain.** *A,* multiple sequence alignment of the junction domains of CDPKs containing a bipartite NLS as a subdomain. The source and corresponding gi numbers are indicated. The relative positions of the subdomains for nuclear localization, pseudosubstrate autoinhibition, and CaMLD binding in the junction domain are indicated. The determinant amino acids for the bipartite NLS are indicated in *red. B,* multiple sequence alignment of the calcium binding EF hand loops of the above CDPKs. The residue numbers important for coordination with calcium in the respective calcium binding loops are indicated. Amino acids deviating from the consensus EF hand loop sequences are indicated in *blue. C,* AtCPK30, a CDPK with NLS in the junction domain, has four consensus EF hands but contains an insertion of 26 amino acids in the border of the catalytic and junction domains. Domain analysis was done using PROSITE. Alignments were developed using ClustalW (35).

1CDM (43) and 1CKK (44) having calmodulin in complexation with target peptides in antiparallel and parallel orientations, respectively, from the Protein Data Bank (45). The peptide templates in 1CDM and 1CKK were used to build the JD. Although the templates used were biomolecular calmodulin-peptide complexes, the target molecule had JD covalently linked to CaMLD. Because of this constraint, the model built using 1CDM showed the presence of knots (the JD peptide traversing through CaMLD). Consequently, the antiparallel mode of peptide binding was ruled out. The model obtained from 1CKK (with the parallel mode of binding) also had a knot with the peptide going through the linker connecting the N- and C-terminal domains of CaMLD (Fig. 8*A*). This could easily be rectified manually. In the second step, the active kinase was built using the sequence of death-associated protein kinase (DAPK) in the Protein Data Bank file 1JKT (46), and this domain, along with the JD-CaMLD model, was used to build the complete structure of CDPK.

The importin-CDPK complex was built by the protein docking method, GRAMM (47), using the structure of importin obtained from importin-NLS peptide complex, Protein Data Bank file 1PJN (48). The interface area between CaMLD and JD was calculated following Ref. 49, and the molecular diagrams were generated using MOLMOL (50).

RESULTS

Domain Analysis of an A. hypogea CDPK and Its Homologs; Nuclear Localization Sequence in the JD Is Coupled with Nonconsensus EF Hand Loops in the CaMLD—We developed a 1.3-kb partial cDNA clone (gi:67479988) of an *Arachis* CDPK (designated AhCPK2) by amplification of RNA prepared from *Arachis* cells that were subjected to osmotic stress (27, 28). The predicted amino acid sequence contains a kinase catalytic domain with subdomains I to XI of Ser/Thr kinases, a junction domain, and a CaMLD with four calcium-binding motifs characteristic of the CDPK family (Fig. 1). Alignment and phylogenetic analysis using the entire length of the deduced AhCPK2 protein sequence showed that it belongs to the branch III cluster of plant and algal CDPKs (3). It showed the highest homology with AtCPK13, an *Arabidopsis* CDPK (gi:28059078) with 86% identity and 94% similarity, and OsCDPK, a rice CDPK (gi:34907990) with 83% identity and 92% similarity. The alignment of AhCPK2 with AtCPK13 and the OsCDPK is shown in Fig. 1.

AhCPK2 also shares 71% identity and 83% similarity with a stress-induced CDPK (AtCPK10) from *Arabidopsis* (51, 52), which appeared consistent with its expression in the stressed *Arachis* cells.

In addition to having the core domain arrangement of a canonical CDPK, AhCPK2 contains a bipartite NLS sequence (PROSITE code no PS00015) in its junction domain, and the sequence of the second calcium binding EF hand loop (PROSITE code PS00018) in its CaMLD was a deviation from the consensus (Fig. 2, *A* and *B*). BLAST search and subsequent domain analysis revealed that several other CDPKs from different species showing strong homology with the *Arachis* CDPK also have a similar domain composition. As indicated in Fig. 2, a coupling was noticed between the presence of a bipartite NLS in the JDs of CDPKs with the absence of one or more calcium binding EF hand loops in their respective CaMLDs.

Multiple sequence alignment revealed that the position of the NLS in the JD of all these CDPKs was superimposable (Fig. 2*A*). Canonical bipartite NLS contains the following: (i) two adjacent basic amino acids (Arg or Lys), (ii) followed by a spacer region of any 10 residues, and (iii) followed by at least three basic residues (Arg or Lys) in the next five positions (21). Comparison of the JD sequences revealed that two of the three basic residues in the C-terminal cluster of the bipartite NLS domain are conserved in all CDPKs (alignment not shown). In fact, this cluster overlaps with the known span of the autoinhibitory subdomain (5–9) in the JD (Fig. 2*A*), which is highly conserved among CDPKs. It is the N-terminal pair of basic residues that is primarily responsible for giving rise to a potential bipartite nuclear localization sequence in the junction domain of the indicated members of the CDPKs.

PS00018 looks for the consensus 12-residue calcium binding EF hand loop D*X*(DNS){ILVFYW}(DENSTG)(DNQGHRK){GP}(LIVMC)(DENQSTAGC)*X*(2)(DE)(LIVMFYW), which is flanked on both sides by a 12-residue α-helical domain (22–26). The calcium ion is coordinated in a pentagonal bipyramidal configuration with six residues in positions 1, 3, 5, 7, 9, and 12 (indicated by *numbers* in Fig. 2*B*). As shown, all except AtCPK10 have a deviation from the consensus in one of these six coordinating residues (Fig. 2*B,* indicated in *blue*). For AtCPK10, the variation is in the 6th residue of the loop, which usually is an invariant glycine and is known to provide the requisite bend of the calcium binding loop structure (22–26). Although some other residues are tolerated in this position, AtCPK10 has a threonine that is not included in the consensus. Also with an exception in AtCPK10, where the third EF hand was predicted to be nonfunctional, the nonconsensus calcium binding loops were present in the N-terminal half of the CaMLDs in all CDPKs of our target group. However, AtCPK13 contained nonconsensus loops both in the N- and C-terminal halves of its CaMLD (Fig. 2*B*).

Although all the above kinases have their NLS sequences in identical positions in their JDs (Fig. 2*A*), a *Plasmodium* kinase (gi:23476982) has an NLS that is not perfectly superimposable. It partially resides in the C terminus of the catalytic domain and partially in the N terminus of its JD. Most interestingly, even this kinase was predicted to have two nonconsensus calcium binding EF hand loop sequences in its CaMLD. Taken together, there is a strict coupling between the presence of an NLS in the JDs of CDPKs with the absence of one or more calcium binding EF hand loops in their respective CaMLDs. AtCPK30 (gi:22655135) was the single exception to the domain coupling phenomenon where, despite having an NLS in the JD, all four calcium binding EF hand loops were predictably functional (Fig. 2*B*). But unlike any other known CDPK, this kinase was found to have a 26-amino acid insertion just preceding the NLS, between the kinase and the junction domain (Fig. 2*C*). This evidence in fact further attests to the fact that the presence of an NLS in the junction domain is accompanied by some sort of a compensatory change in the total kinase.

Calcium Binding Property of the Arachis CDPK—PROSITE analysis indicated the second EF hand loop of the CaMLD of the *Arachis* CDPK to be nonfunctional. This is because among the six residues in positions 1, 3, 5, 7, 9, and 12 that are known to coordinate with calcium in a standard 12-residue EF hand loop structure, two residues at positions 1

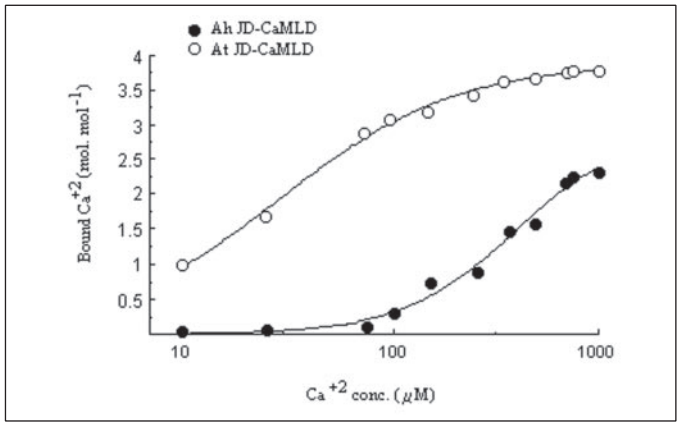

FIGURE 3. **Calcium binding property of AhCPK2.** The JD-CaMLD polypeptide of AhCPK2 with a nonconsensus EF hand loop in the second calcium-binding site was investigated for calcium binding by equilibrium dialysis according to the "Experimental Procedures." The figure represents the best fit to the obtained calcium binding data using the Hill model (37, 38). Under similar conditions, the calcium binding property of the JD-CaMLD polypeptide of AtCPK1 with four consensus EF hands has been investigated as a reference.

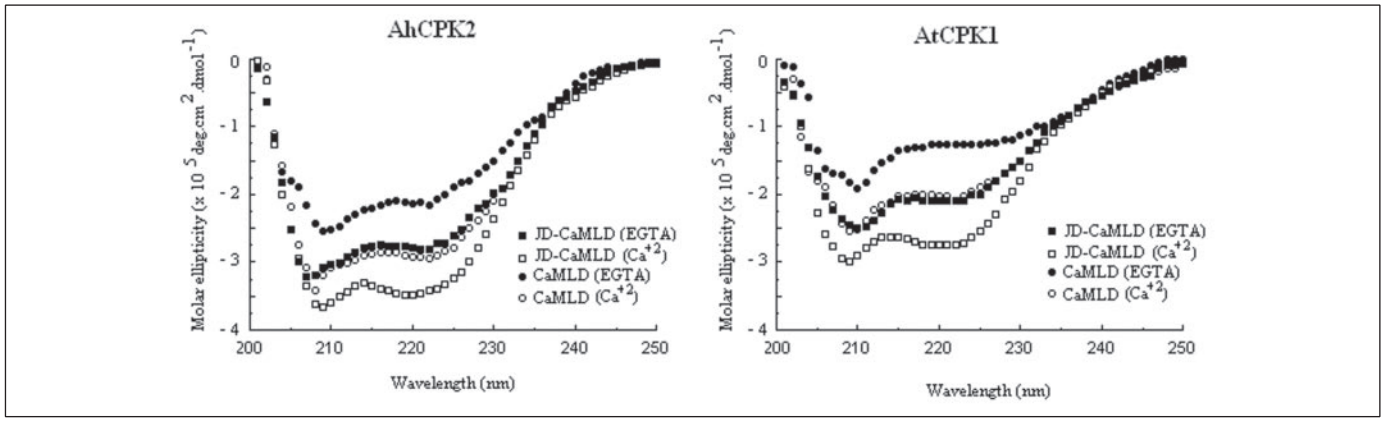

FIGURE 4. **Far-UV CD spectra of the regulatory apparatus of AhCPK2.** The spectra were developed for the JD-CaMLD and the CaMLD polypeptides of the *Arachis* CDPK AhCPK2 with a nonconsensus EF hand loop in the second calcium-binding site. Spectra were recorded with 5 μM protein in 20 mM Tris-HCl, pH 7.4, in the presence of 1 mM Ca^{2+} or 5 mM EGTA. Under similar conditions, the spectra were also recorded for the JD-CaMLD and the CaMLD polypeptide of AtCPK1 with four consensus EF hands as a reference.

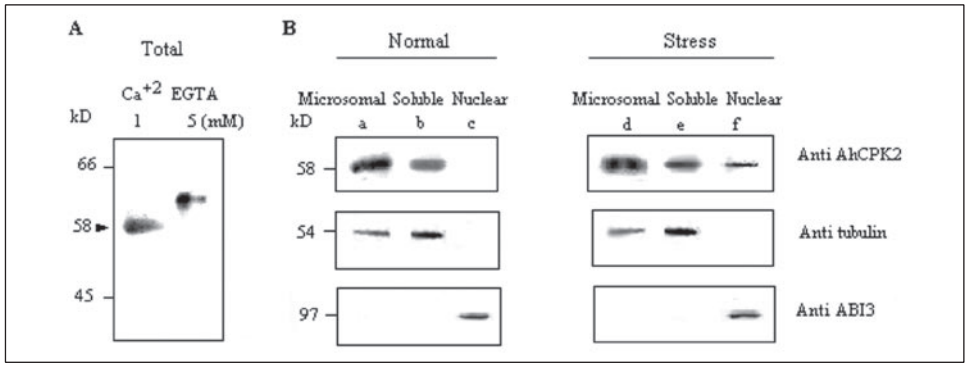

FIGURE 5. **Subcellular localization of the endogenous form of AhCPK2.** The endogenous form of AhCPK2 was detected in *Arachis* cell extracts using anti-AhCPK2. *A,* Western blot analysis of total protein preparation treated with either calcium or EGTA. Cross-reactive bands are indicated. *B,* Western blot analysis of the microsomal, soluble, and the nuclear protein preparation from normal and stressed *Arachis* cells using anti-AhCPK2, anti-tubulin, and anti-ABI3.

and 5 deviated from the consensus. To understand the effect of such a deviation, we investigated the calcium binding properties of the JD-CaMLD polypeptide of the *Arachis* CDPK, and we compared it with its canonical counterpart obtained from an *Arabidopsis* CDPK AtCPK1 (32) where all four EF hand loops follow the consensus pattern (Fig. 3). Binding of calcium was measured by equilibrium dialysis according to Refs. 36 and 53. The binding parameters were evaluated by analyzing the experimental data based on the Hill model of cooperative binding to equivalent binding sites. The binding capacity of the *Arachis* JD-CaMLD polypeptide was determined to be 3.1 mol of calcium/mol of protein at saturation, and the K_d value was determined to be 392 μM. Under identical conditions the JD-CaMLD of AtCPK1 could bind 3.8 mol of calcium/mol of the polypeptide with a K_d value of 0.19 μM. The calcium binding property of the *Arachis* CDPK thus appears to be significantly deviated from those of the canonical CDPKs and is very consistent with the PROSITE prediction of a nonconsensus calcium binding EF hand loop in its CaMLD region. It may be noted that *Plasmodium* CDPK with mutations in the first or second calcium binding loop had its K_d values raised to the 200–330 μM range (53), which is similar to the values obtained with the *Arachis* CDPK. The value of the Hill constant (degree of cooperativity) was found to be greater than 1, in calcium binding to *Arachis* JD-CaMLD, indicating that there is a positive cooperativity in calcium binding to this polypeptide. Such cooperativity in calcium binding is a common feature of all calmodulin-like proteins (32, 53).

Global Fold of the Calcium-responsive CDPK Regulatory Apparatus (32) Remains Unchanged in the Arachis CDPK—The CaMLD polypeptides from canonical CDPKs are found to be highly helical in nature with the helicity increasing further in response to calcium (32, 54). In the corresponding JD-CaMLD polypeptides, interaction of the JD with the CaMLD leads to a further increase in helicity, and this change is attributed to the helical character of the JD developed as a consequence of its binding to CaMLD as well as the change in spatial distribution of the helices in the CaMLD region that moves from disordered to an ordered structure (32). To understand how the deviation in the calcium binding would affect the characteristic structural response of the *Arachis* CDPK (AhCPK2), we followed the calcium-responsive structural change of the CaMLD and the JD-CaMLD region of this kinase, and we compared it with its canonical counterparts obtained from an *Arabidopsis* kinase AtCPK1 (32), by studying the far-UV CD spectrum of the corresponding polypeptides.

The spectra of CaMLD and the JD-CaMLD polypeptides from AhCPK2 as well as AtCPK1 had dominant contributions from the helical secondary structure with the minima at 208 and 222 nm (Fig. 4). For both the polypeptides with each of these kinases there was an increase in intensity upon addition of calcium. Also, in both cases there was a considerable increase in the helical component of the JD-CaMLD polypeptide as compared with the corresponding CaMLD, which was suggested earlier to be due to the helical character of the junction region in the JD-CaMLD polypeptide (32). This analysis broadly suggests that at saturating concentrations of calcium, the global fold of the regulatory apparatus in the *Arachis* CDPK remains similar to its canonical counterpart despite having wide differences in their calcium binding properties. The activation principle of the *Arachis* CDPK thus appears to follow the known activation principles for CDPKs (7–9).

Subcellular Localization of the Endogenous Arachis CDPK—The JD-CaMLD region of the *Arachis* CDPK contained unique features that distinguished it from canonical CDPKs (Fig. 2). Therefore, to detect the endogenous polypeptide representing the untagged or native *Arachis* CDPK (AhCPK2) in the cultured *Arachis* cells, we raised polyclonal antibodies against the JD-CaMLD polypeptide of the kinase. This antibody cross-reacted with a single 58-kDa band in the total protein preparation of the *Arachis* cells that showed a characteristic calcium-dependent shift in mobility (Fig. 5*A*). It failed to cross-react with the 53-kDa CDPK in dry seed extracts of *A. hypogea* that we previously characterized (55, 56), thus indicating the specificity of its interaction (data not shown). As AhCPK2 was originally isolated from osmotically stressed cells, we used both normal and stressed cells for our detection experiments. The cells were resolved into soluble and microsomal fractions or into a nuclear fraction by isolating intact nuclei, and the isolated proteins from these fractions were subjected to Western blot analysis using the raised antibody. The cross-reactive 58-kDa polypeptide was localized in the microsomal fractions (Fig. 5*B, lanes a* and *d*) and the soluble fractions (*lanes b* and *e*) in both the normal and the stressed cells, indicating the kinase to be distributed in both membrane and soluble fractions. The kinase was not detectable in the nuclear fraction of the normal cells (Fig. 5*B, lane c*), but it was clearly detectable in the nuclear fraction of the stressed cells that were subjected to 0.4 M sucrose for 4 days (Fig. 5*B*, *lane f*). These *Arachis* cells have a unique stress physiology. In the presence of stress they are driven to quiescence, but an hour of auxin treatment completely restores their growth potential (27–29). The subcellular localization of AhCPK2 remains unchanged following auxin treatment in these *Arachis* cells (data not shown). These observations suggest that AhCPK2 responds to stress-originated signals by being localized in the nucleus. Similar dynamicity in subcellular localization in response to stress has been noted earlier with McCPK1, a CDPK from *Mesembryanthemum crystallinum* (57). Anti-tubulin antibody cross-reacted with the soluble and the microsomal protein preparations (58) but showed no cross-reaction with the nuclear protein, indicating our fractionation procedures were effective (Fig. 5*B*). Antibodies raised against the transcription factor ABI3 (abscisic acid-insensitive 3) that is induced in presence of auxin in these cells (29) are,

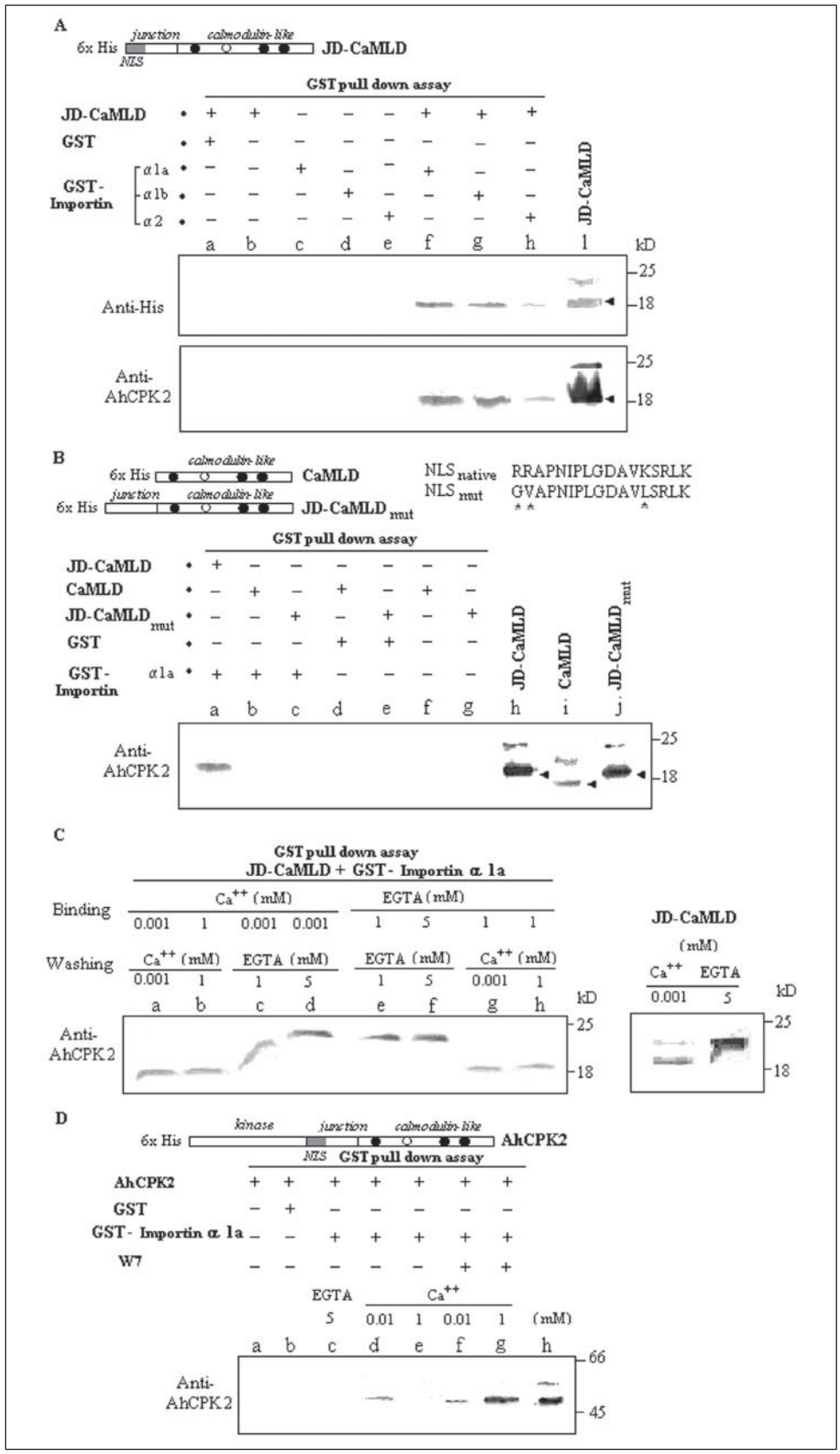

FIGURE 6. **Importin binding property of AhCPK2.** Importin binding was investigated by GST pull-down assay as described under "Experimental Procedures." GST-tagged proteins were precipitated from the reaction mixtures using glutathione-Sepharose 4B beads, and the importin-bound proteins were detected by Western blot analysis with anti-His or anti-AhCPK2 as indicated. *A,* the His-tagged JD-CaMLD polypeptide was subjected to binding with GST (*lane a*) or the indicated GST-tagged importins (*lanes f, g,* and *h*). The compositions of the necessary control reaction mixtures are indicated in the figure (*lanes b–e*). *Lane l* contains a standard JD-CaMLD polypeptide without being subjected to binding reactions. The positions of the calcium-bound JD-CaMLD in both panels are indicated by *arrowheads. B,* the His-tagged JD-CaMLD, CaMLD, and JD-CaMLD$_{mut}$ was subjected to binding with GST-tagged importin α1a (*lanes a–c*). The compositions of the necessary control reaction mixtures are indicated in the figure (*lanes d–g*). *Lanes h–j* contain standard JD-CaMLD, CaMLD, and JD-CaMLD$_{mut}$ polypeptide without being subjected to binding reactions. The positions of calcium bound polypeptides are indicated by *arrowheads.* The mutated residues in JD-CaMLD$_{mut}$ are indicated by *asterisks. C,* binding of GST-importin α1a with His$_6$ JD-CaMLD of AhCPK2 was investigated in the presence of the indicated concentrations of calcium (*lanes a–d*) or EGTA (*lanes e–h*). Subsequent to binding under the indicated conditions, the glutathione beads were subjected to washing in the presence of the indicated concentrations of calcium (*lanes a, b, g,* and *h*) or EGTA (*lanes c–f*). The characteristic shift of electrophoretic mobility of JD-CaMLD polypeptide in the presence and absence of calcium is shown in the adjacent panel. *D,* the His-tagged AhCPK2 polypeptide was subjected to binding with GST-tagged importin α1a (*lanes c–g*). The compositions of the necessary control reaction mixtures are indicated (*lanes a* and *b*). Binding was investigated in the presence of the indicated concentrations of EGTA (*lanes c*) and calcium (*lanes d–g*) in the presence (*lanes f* and *g*) or in the absence (*lanes d* and *e*) of 2 mM W7. *Lane h* contains standard AhCPK2 polypeptide without being subjected to binding reactions.

however, strictly localized in the nuclear fractions of the *Arachis* cells (Fig. 5*B*, *lanes c* and *f*). Such detection of the *Arachis* CDPK (AhCPK2) in the nuclear fraction of the stressed *Arachis* cells is consistent with the PROSITE prediction of an NLS in its JD.

Presently, functional annotation available for our target set of CDPKs having an NLS sequence in JD is low, and nuclear localization has not been reported for any of them. In fact, AtCPK7 and AtCPK8, members of our target group, have been localized in membranes but not in the

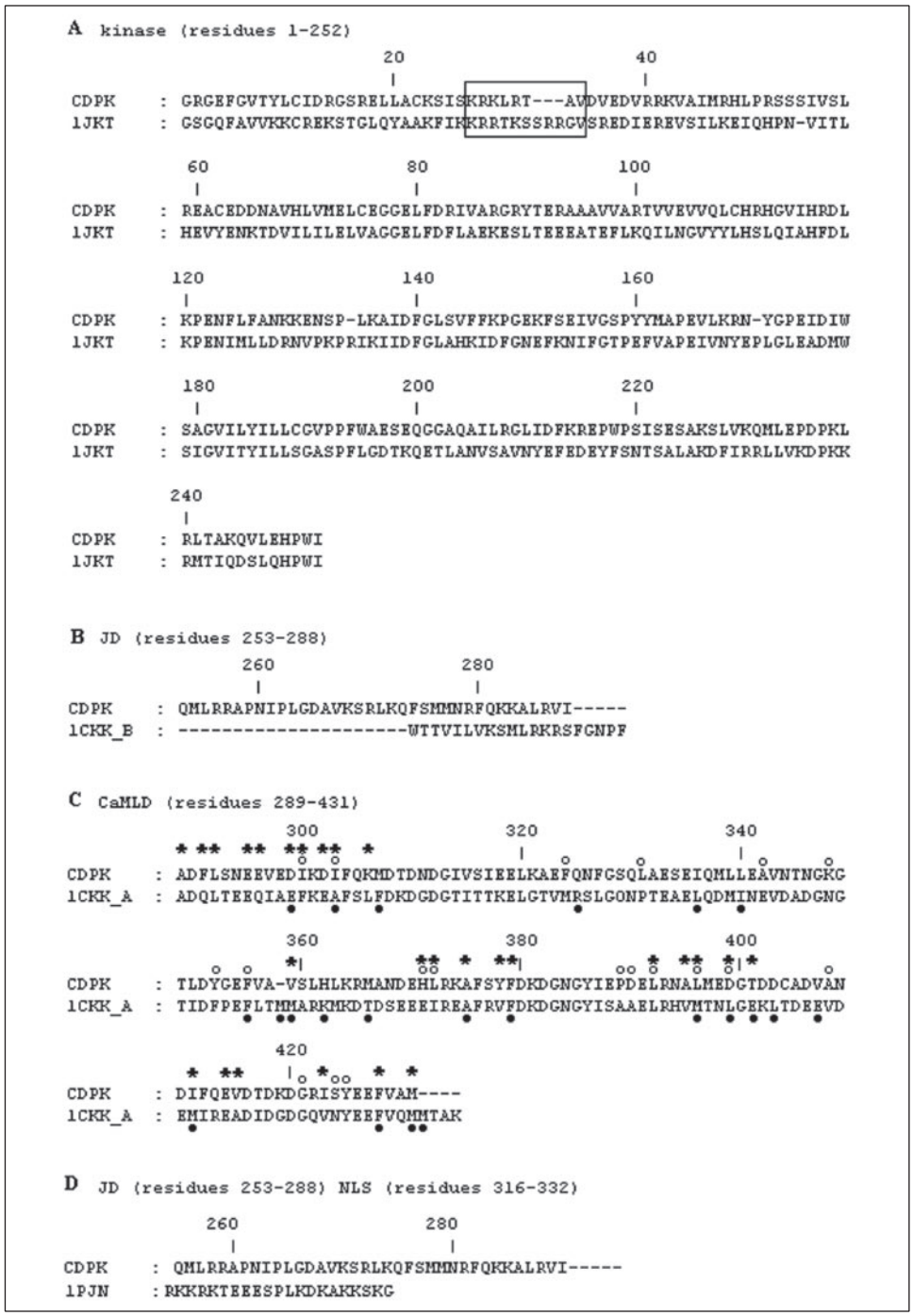

FIGURE 7. **Sequence alignment of AhCPK2 with the requisite templates used for homology modeling of various domains.** Alignments are shown for the catalytic domain of AhCPK2 with the death-associated protein kinase (*DAPK*) in 1JKT; a basic loop conserved in DAPK family is indicated in a *box* (*A*). *B,* CaMLD binding region in JD of AhCPK2 with calmodulin-bound target peptide in 1CKK. *C,* CaMLD of AhCPK2 with calmodulin in 1CKK; *asterisks* indicate residues in the CaMLD of AhCPK2 that are proposed to be interacting with its JD in the structure, built by us; *black circles* indicate residues involved in target interaction in calmodulin in the 1CKK structure (44); *open circles* indicate residues involved in JD interaction in CaMLD of the 1S6I structure (66). *D,* NLS sequence in JD of AhCPK2 with the NLS sequence in 1PJN. The range of the domains of the modeled structure is given in *parentheses*. All alignments are done using ClustalW (35) with one minor modification in the region between EF hands 2 and 3 in *C*, following Ref. 54.

nucleus (17). Similar to what has been observed with the *Arachis* CDPK, it is possible that specific signatures of stress-associated calcium signaling have a role in localizing these kinases in the nucleus. Alternatively, as suggested by the authors (17), it is also possible that addition of a C-terminal green fluorescent protein tag has interfered with proper targeting of these kinases. Another *Arabidopsis* CDPK, AtCPK13, was shown previously to contain an NLS (PlantsP no. 84110) in its JD, but we were intrigued to find that in its recent curated form (PlantsP no. 137883) the NLS has been removed from its annotation.

Importin Binding as Evidence for the Presence of NLS in the Junction Domain of the Arachis CDPK—The bipartite NLS motifs are known to bind importins, the shuttle proteins of the nuclear transporting machinery through their positive residues (59, 60). We used this importin binding property for demonstrating the presence of NLS in the JD region of the JD-CaMLD polypeptide from the *Arachis* CDPK. GST pull-down assays were done to check the binding between GST-tagged importin α1a, α1b, and α2 proteins from rice (33, 61) and the His_6-tagged JD-CaMLD polypeptide from the *Arachis* CDPK. Both anti-His and antibodies raised against the JD-CaMLD polypeptide of AhCPK2 were used for detecting the importin-bound polypeptide by Western blot analysis (Fig. 6*A*). In standard binding conditions the JD-CaMLD polypeptide could be detected in the pulled down complexes associated with all three importins α1a, α1b, or α2, indicating a successful binding between the JD-CaMLD polypeptide and the importins (Fig. 6*A*, *lanes f–h*). To ascertain that the binding of JD-CaMLD polypeptide with importin is mediated through the JD, we undertook similar binding reactions under

identical conditions with the CaMLD polypeptide and the importin α1a. As indicated in Fig. 6*B*, *lane b*, the CaMLD polypeptide was not detected in association with importin α1a, indicating the observed binding of the JD-CaMLD (Fig. 6*B, lane a*) polypeptide to be specific for the JD region that contains the NLS. To further ascertain that the NLS sequence in the JD is important for binding with importin, we undertook binding assays with a mutated variant of the JD-CaMLD where three important determinants of NLS, namely Arg-256, Arg-257, and Lys-268, have been replaced with Gly, Val, and Leu, respectively. This mutated polypeptide was not detected in association with importin α1a (Fig. 6*B, lane c*) indicating the binding of the JD-CaMLD (Fig. 6*B, lane a*) polypeptide was mediated through the NLS sequence present in the JD region of the kinase. Under identical conditions GST protein *per se* failed to show any binding with the JD-CaMLD, CaMLD, and the JD-CaMLD$_{mut}$ polypeptides (Fig. 6, *A*, *lane a,* and *B, lanes d* and *e*), indicating that the observed bindings of GST-importins were importin-mediated. Thus the junction domain of AhCPK2 was demonstrated to have a nuclear localization sequence through its ability to interact with the importin proteins of the nuclear transport machinery.

We then checked whether binding of importin to the junction domain was affected by the intramolecular interaction within the JD-CaMLD polypeptide in the presence of calcium. For this, binding reactions were set up with GST-importin α1a and His$_6$ JD-CaMLD of AhCPK2 in the presence of the indicated concentrations of calcium or EGTA (Fig. 6*C*). As indicated, the presence or absence of calcium did not interfere with the interaction of JD-CaMLD with importin. Depending on the presence of calcium or EGTA during washing, the JD-CaMLD polypeptide was detected in its calcium-bound or unbound form with a characteristic shift of electrophoretic mobility (Fig. 6*C*). Thus, without the constraints of having the catalytic domain around in the JD-CaMLD polypeptide, interaction of the NLS with importin appeared to be calcium-insensitive.

Our attempts to demonstrate importin binding with the whole kinase, where the NLS in the JD is sandwiched between the catalytic and the CaMLD domains, was unsuccessful irrespective of whether we did our binding assays in the presence of saturating concentrations (1 mM) of calcium (Fig. 6*D*, *lane e*) or in the absence (5 mM EGTA) of calcium (*lane c*). Most interestingly, when we tested the calcium dependence of the whole kinase-importin interaction, successful binding was noted at low concentrations (10 μM) of calcium (Fig. 6*D, lane d* and *f*). In addition, we could also detect effective binding of importin with the whole kinase in the presence of 1 mM calcium when W7 was included in the binding reaction (Fig. 6*D, lane g*). It appears that at low calcium concentrations, the CaMLD successfully maneuvers the withdrawal of the autoinhibitory domain from the clutches of the catalytic domain, but it does not interact with JD in a manner that would bury the autoinhibitory domain. Therefore, the adjacently placed NLSs in the JD remain accessible to importins under such conditions. On a similar note, we reasoned that in the presence of saturating concentrations of calcium, interaction of JD with the CaMLD completely sandwiched the NLS between the catalytic and the CaMLD structure and thus hindered its interaction with importin. But under the same conditions in the presence of W7, prohibition of the proper interaction of the JD with the CaMLD allows interaction of importin with the NLS.

Three-dimensional Model of Interaction of Arachis CDPK with Importin—To visualize the interaction of importin with the full-length kinase, we developed a model for the binary complex between the whole structure of the *Arachis* CDPK and importin through homology modeling and docking. No protein structure is available with JD and CaMLD covalently linked. Therefore, we took recourse in the available three-

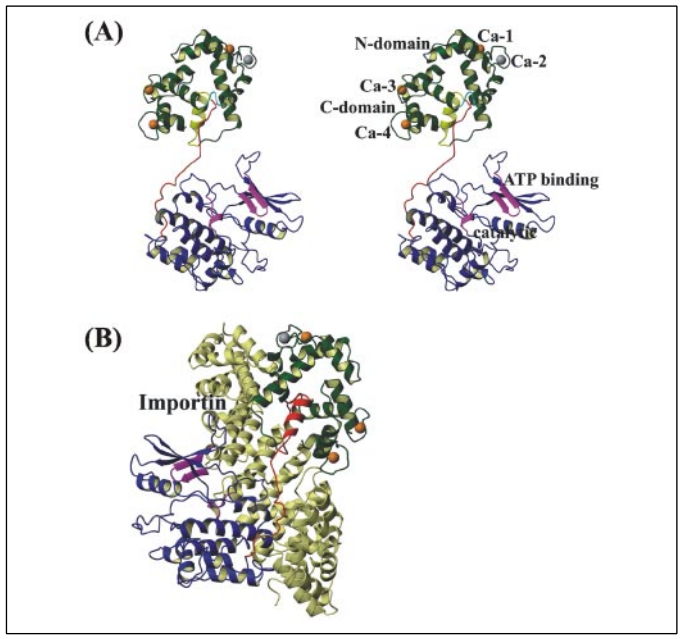

FIGURE 8. **Homology model of AhCPK2 and its interaction with importin.** *A,* stereo view of the ribbon model of AhCPK2. The color coding is as follows: kinase, *blue*; CaMLD, *green*; CaMLD binding region of JD, *yellow*; NLS in JD, *red*; three calcium ions located in the canonical binding sites, *orange*; remaining one, which could be defective, *gray*; catalytic and ATP-binding sites, *magenta. B,* ribbon diagram of the AhCPK2-importin complex. Importin is shown in *yellow-white,* and JD is in *red*; the other color codes are as in *A*.

dimensional structures of binary complexes of calmodulin and target peptides. Considerable efforts have gone into understanding target recognition by CaM using synthetic peptide analogs of CaM binding regions (43, 44, 62–64). Generally, the peptide can be positioned in the peptide-binding channel of CaM in two relative orientations, parallel or antiparallel depending on whether the N-terminal region of the peptide is closer to the N-terminal or the C-terminal domain of CaM/CaMLD. As discussed under "Experimental Procedures," the parallel mode of binding appeared to be more plausible for interaction of JD with CaMLD. The alignments of sequences of the target peptide and CaM in 1CKK with the JD and CaMLD sequences of *Arachis* CDPK are shown in Fig. 7, *B* and *C,* respectively. Next, we developed a model for the active conformation of the *Arachis* CDPK catalytic domain using the crystal structure (Protein Data Bank code 1JKT) (46) of DAPK (34% identity and 37% similarity) (Fig. 7*A*) and joined it with the JD-CaMLD to construct the complete structure (Fig. 8*A*).

The surface area that is buried as the peptide forms a complex with CaM in 1CKK is 3448 Å^2, but in our model of JD-CaMLD it is much smaller (1687 Å^2). It is possible that because JD is covalently linked to the N-terminal end of CaMLD in CDPK, the CaMLD binding region (the helical part of JD) cannot go deep into the channel, thus remaining partially exposed. In our model, the CaMLD binding region is shared evenly between the two domains, the interface area being 915 and 773 Å^2 with the N- and C-terminal domains, respectively. However, more residues (His-371, Leu-372, Ala-375, Tyr-378, Phe-379, Leu-392, Ala-395, Leu-396, Asp-399, Thr-401, Ile-411, Glu-414, Val-415, Ile-423, Phe-428, and Met-431, for a total of 16) are contributed by the C-terminal domain than the N-terminal domain (Ala-289, Asp-290, Phe-291, Leu-292, Glu-295, Glu-296, Asp-299, Ile-300, Asp-302, Ile-303, Lys-306, and Val-359, for a total of 12). This is consistent with the prevailing understanding about JD and CaMLD interaction, where the C-terminal lobe is documented to be involved in direct binding of the target in JD (32). We have compared the residues (Fig. 7*C, asterisks*) in CaMLD of *Arachis* CDPK that are

found to be interacting with its JD in our model with the residues (*black circles*) involved in target interaction in CaM in 1CKK (44) and also the residues (*open circles*) involved in JD interaction in CaMLD of the structure 1S6I (66). As can be seen, there is a considerable overlap in the residues and regions of CaMLD that appeared to be interacting with JD in our model with those found to be interacting in similar structures.

The proposed structure (Fig. 8*A*) has two domains with the terminal catalytic (*blue*) and CaMLD (*green*) domains linked by JD, which has mainly an irregular structure (*red*) with a helical region (*yellow*) that interacts with the CaMLD. The NLS region of the JD (Fig. 8*A*, *red*) is exposed in the structure and appears amenable to interact with its cognate receptors or importins. The active site of the kinase (Fig. 8*A*, *magenta*) is spatially away from the NLS, and consequently the binding of importin at the NLS may not block the catalytic function of the activated kinase. The importin-CDPK complex structure (Fig. 8*B*) also shows that importin binding should not interfere with the kinase activity. It may be mentioned that although there is considerable sequence similarity (Fig. 7*D*), we did not use the NLS in 1PJN as template when building this region. Still, NLS was modeled to have extended, nonregular conformation, as observed for the NLS peptide in 1PJN. Additionally, GRAMM (47), which is a surface-recognition program, also identifies NLS as the docking site in AhCPK2, and the overall fitting is very snug. Although it is difficult to comment on the exact conformation of NLS and the relative orientation of the kinase and CaMLD domains in the absence of importin, the model in Fig. 8*B* depicts the feasibility of a successful interaction of the *Arachis* CDPK with importin and is consistent with our biochemical data, where binding of several importins has been demonstrated with the kinase.

DISCUSSION

We note that the presence of nuclear localization sequences in the junction domain of CDPKs is obligatorily coupled with nonfunctional EF hand loops in their respective CaMLDs (Fig. 2). Thus this subgroup of noncanonical CDPKs represents a unique and discrete case where interdomain compensatory changes are accompanied with a domain evolution (67, 68). The precise question that arises is why atypical calcium binding property was a primary requisite for acquiring a functional NLS in junction domains of CDPKs. We discuss our results on a CDPK from *A. hypogea*, a member of our target group of noncanonical CDPKs, and propose a possible explanation for such obligatory domain coupling in the light of the known mechanism of activation of canonical CDPKs (7–9, 32).

The *Arachis* CDPK has a deviation from the consensus in its second calcium-binding site and has been shown to have significantly low affinity for calcium (K_d 392 μM) as compared with a canonical CDPK (K_d 0.19 μM) (32). However, despite having wide differences in their calcium binding properties (Fig. 3), the change in secondary structure for the *Arachis* CDPK at saturating concentrations of calcium was exactly similar to its canonical counterparts (Fig. 4) (32). These observations are very similar to an earlier report on a *Plasmodium* CDPK where mutations in calcium-binding sites of the N-terminal lobe of its CaMLD significantly decreased its affinity for calcium, but the accompanied change in secondary structure of these mutant kinases resembled the wild type at saturating calcium concentrations (1–10 mM).

Because the characteristic calcium-dependent structural response in the CaMLDs is reported to be associated with the regulatory apparatus of canonical CDPKs (7–9), the principle of activation of the *Arachis* CDPK appear to remain unchanged. Canonical CDPKs are activated by the cumulative effect of two calcium-responsive structural changes. (i) At low calcium levels high affinity binding sites in the C-terminal lobe are occupied and it interacts with the JD. (ii) When calcium levels rise to fill the two weaker binding sites in the N-terminal lobe, it triggers a conformational change through the tether region. Such interdomain complex interactions form a collapsed structure that leads to exposition of the catalytic site and activation (9, 32). Because in our target group of CDPKs the nonconsensus calcium-binding sites are detected predominantly in the N-terminal lobe, the tether-mediated activation through its low affinity calcium-binding sites is most likely to be inactivated at subsaturating concentrations of calcium. Under similar conditions the interaction of JD with the C-terminal lobe of CaMLD with high affinity binding sites is unlikely to be affected (53).

In the light of this known mechanism of activation of CDPKs, we next discuss the atypical calcium binding properties of the *Arachis* CDPK in relation to its possible role in the functional exposition of the NLS present in its JD. A known mechanism for regulating the activity of NLS is masking it in order to prevent its recognition by importins (69, 70). It is interesting to note that by virtue of having the NLS in the junction domain with a partial overlap with the autoinhibitory sequence, our target group of CDPKs can have their NLS masked by the catalytic domain in the inactive form of the kinase (7–9, 32). Through *in vitro* binding assays the interaction of importin with the *Arachis* CDPK could only be detected at subsaturating (10 μM) concentrations of calcium (Fig. 6*D*). As per the literature, under such conditions the interaction of the JD with the C-terminal lobe of CaMLD remains unaffected, which therefore can withdraw the autoinhibitory sequence from the catalytic groove of the kinase. Such interdomain rearrangements allow the functional exposure of the NLS sequence in the JD and its subsequent interaction with the nuclear transport factors (Fig. 6*D*). Through similar binding assays, we could not detect any interaction of importin with the *Arachis* CDPK at saturating concentrations of calcium. Under such conditions the low affinity calcium-binding sites are occupied in the N-terminal lobe, which triggers a conformational change that appears to bury the JD in the CaMLD in such a manner that the NLS becomes inaccessible to importins (Fig. 6*D*). Such a proposition was confirmed when we found importin to interact with the *Arachis* kinase at saturating concentrations of calcium in presence of W7 that prevented the interaction of JD with the CaMLD (Fig. 6*D*). The discrete differences in importin binding with the *Arachis* CDPK at saturating and subsaturating calcium concentrations suggest the kinase to have an intermediate structure at a low calcium signature that is capable of interacting with importin. Such a proposition for a calcium-dependent intermediate structure is consistent with the observations made by Zhao *et al.* (53) on a *Plasmodium* CDPK. They noticed that conformational change in the wild type kinase was complete at subsaturating concentrations of calcium (100 μM), but in mutant kinase where calcium-binding sites were defective in the N-terminal lobe of its CaMLD, the full conformational change required a very high calcium concentration (53). This clearly indicated that CDPKs with nonfunctional EF hand motifs in their N-terminal lobe gradually attain their requisite change in structure in response to an increase in calcium concentration.

Finally, it appears that by virtue of having atypical calcium binding properties, our target group of CDPKs can sense a specific low calcium signature that helps in functional exposition of the NLS in the JD because of noncanonical interaction between the JD and its CaMLD. In response to the same signature, canonical CDPKs with four consensus calcium-binding sites are expected to have successful intramolecular interaction of JD with their respective CaMLDs, and this would prevent access of importin to its JD. This probably justifies the coupling between

a nonconsensus calcium-binding site in a CDPK with the presence of an NLS in its JD. It is possible that importin binding compensates for the absence of the tether constraint and provides the extra force for activation of these noncanonical kinases. This is significant because it would ensure that the kinase did not become active without ensuring its localization inside the nucleus.

It may be noted that the calcium dependence of the enzymatic activity of the *Arachis* CDPK could not be studied as it failed to phosphorylate any known exogenous substrate.[6] Most interestingly, AtCPK10 which, similar to the *Arachis* CDPK, is associated with stress-dependent signaling events and is a member of our target group, also failed to phosphorylate any exogenous substrate (51). The evidence suggests that this subgroup of noncanonical CDPKs is active against unique substrates that have yet to be identified. It was interesting to note that a basic loop, which is believed to be a characteristic feature of the DAPK family (based on which the homology model of the *Arachis* CDPK in Fig. 8*A* was built), is partially conserved in the *Arachis* CDPK (indicated by a *box* in Fig. 7*A*). This loop is believed to have a role in strictly restricting the choice of substrate in the enzymes (46, 65), and the physiological substrate of this apoptosis-related kinase has yet to be identified. Further investigations are needed for the identification of the physiological substrates of our target kinases and for understanding the true significance of the observed domain coupling.

Acknowledgments—We thank Prof. Jeffery Harper, Department of Biochemistry and Molecular Biology, University of Nevada, for providing the JD-CaMLD and CaMLD clones of AtCPK1 and Prof. Toshisuke Iwasaki, Department of Biology, Niigata University, Japan, for providing the clones of rice GST-importin α1a, α1b, and α2. The computational modeling was supported by the Department of Biotechnology, Government of India.

REFERENCES

1. Harper, J. F., Sussman, M. R., Schaller, E. G., Putnam-Evans, C., Charbonneau, H., and Harmon, A. C. (1991) *Science* **252,** 951–954
2. Cheng, S. H., Willmann, M. R., Chen, H. C., and Sheen, J. (2002) *Plant Physiol.* **129,** 469–485
3. Harmon, A. C., Gribskov, M., and Harper, J. F. (2000) *Trends Plant Sci.* **5,** 154–159
4. Zhang, X. S., and Choi, J. H. (2001) *J. Mol. Evol.* **53,** 214–224
5. Harper, J. F., Huang, J. F., and Lloyd, S. J. (1994) *Biochemistry* **33,** 7267–7277
6. Harmon, A. C., Yoo, B. C., and McCaffery, C. (1994) *Biochemistry* **33,** 7278–7287
7. Huang, J. F., Teyton, L., and Harper, J. F. (1996) *Biochemistry* **35,** 13222–13230
8. Yoo, B. C., and Harmon, A. C. (1996) *Biochemistry* **35,** 12029–12037
9. Vitart, V., Christodoulou, J., Huang, J. F., Chazin, W. J., and Harper, J. F. (2000) *Biochemistry* **39,** 4004–4011
10. Kobe, B., and Kemp, B. E. (1999) *Nature* **402,** 373–376
11. Asano, T., Tanaka, N., Yang, G., Hayashi, N., and Komatsu, S. (2005) *Plant Cell Physiol.* **46,** 356–366
12. Dammann, C., Ichida, A., Hong, B., Romanowsky, S. M., Hrabak, E. M., Harmon, A. C., Pickard, B. G., and Harper, J. F. (2003) *Plant Physiol.* **132,** 1840–1848
13. Lu, S. X., and Hrabak, E. M. (2002) *Plant Physiol.* **128,** 1008–1021
14. Anil, V. S., Harmon, A. C., and Rao, K. S. (2000) *Plant Physiol.* **122,** 1035–1044
15. Pical, C., Fredlund, K. M., Petit, P. X., Sommarin, M., and Moller, I. M. (1993) *FEBS Lett.* **336,** 347–351
16. Patharkar, O. R., and Cushman, J. C. (2000) *Plant J.* **5,** 679–691
17. Hrabak, E. M., Chan, C. W. M., Gribskov, M., Harper, J. F., Choi, J. H., Halford, N., Kudla, J., Luan, S., Nimmo, H. G., Sussman, M. R., Thomas, M., Walker-Simmons, K., Zhu, J. K., and Harmon, A. C. (2003) *Plant Physiol.* **132,** 666–680
18. Dingwall, C., and Laskey, R. A. (1986) *Annu. Rev. Cell Biol.* **2,** 367–390
19. Garcia-Bustos, J. F., Heitman, J., and Hall, M. N. (1991) *Biochim. Biophys. Acta* **1071,** 83–101
20. Gomez-Marquez, J., and Segade, F. (1988) *FEBS Lett.* **226,** 217–219
21. Dingwall, C., and Laskey, R. A. (1991) *Trends Biochem. Sci.* **16,** 478–481
22. Kawasaki, H., and Kretsinger, R. H. (1995) *Protein Profile* **2,** 297–490
23. Kretsinger, R. H. (1987) *Cold Spring Harb. Symp. Quant. Biol.* **52,** 499–510
24. Moncrief, N. D., Kretsinger, R. H., and Goodman, M. (1990) *J. Mol. Evol.* **30,** 522–562
25. Nakayama, S., Moncrief, N. D., and Kretsinger, R. H. (1992) *J. Mol. Evol.* **34,** 416–448
26. Heizmann, C. W., and Hunziker, W. (1991) *Trends Biochem. Sci.* **16,** 98–103
27. Seal, A., Hazra, A., Nag, R., Chaudhuri, S., and DasGupta, M. (2001) *Plant Cell Rep.* **20,** 567–573
28. Nag, R., Maity, M. K., Seal, A., Hazra, A., and DasGupta, M. (2005) *Plant Cell Tissue Org. Cult.* DOI: 10.1007/s11240-005–6902-z
29. Nag, R., Maity, M. K., and DasGupta, M. (2005) *Plant Mol. Biol.* **59,** 819–836
30. Laemmli, U. K. (1970) *Nature* **227,** 680–685
31. Bradford, M. M. (1976) *Anal. Biochem.* **72,** 248–254
32. Christodoulou, J., Malmendal, A., Harper, J. F., and Chazin, W. J. (2004) *J. Biol. Chem.* **279,** 29092–29100
33. Jiang, C., Imamoto, N., Matsuki, R., Yoneda, Y., and Yamamoto, N. (1998) *J. Biol. Chem.* **273,** 24083–24087
34. Hulo, N., Sigrist, C. J. A., Le Saux, V., Langendijk-Genevaux, P. S., Bordoli, L., Gattiker, A., De Castro, E., Bucher, P., and Bairoch, A. (2004) *Nucleic Acids Res.* **32,** D134–D137
35. Thompson, J. D., Higgins, D. G., and Gibson, T. J. (1994) *Nucleic Acids Res.* **22,** 4673–4680
36. Potter, J. D., Strang-Brown, P., Walker, P. L., and Iida, S. (1983) *Methods Enzymol.* **102,** 135–143
37. Dahlquist, F. W. (1978) *Methods Enzymol.* **48,** 270–299
38. Cornish-Bowden, A., and Koshland, D. E. J. (1975) *J. Mol. Biol.* **95,** 201–212
39. Chico, J. M., Raices, M., Tellez-Inon, M. T., and Ullora, R. M. (2002) *Plant Physiol.* **128,** 256–270
40. Harlow, E., and Lane, D. (1988) *Antibodies: A Laboratory Manual,* pp. 53–138, Cold Spring Harbor Laboratory Press, Cold Spring Harbor, NY
41. Frangioni, J. V., and Neel, B. G. (1993) *Anal. Biochem.* **210,** 179–187
42. Marti-Renom, M. A., Stuart, A., Fiser, A., Sánchez, R., Melo, F., and Sali, A. (2000) *Annu. Rev. Biophys. Biomol. Struct.* **29,** 291–325
43. Meador, W. E., Means, A. R., and Quiocho, F. A. (1993) *Science* **262,** 1718–1721
44. Osawa, M., Tokumitsu, H., Swindells, M. B., Kurihara, H., Orita, M., Shibanuma, T., Furuya, T., and Ikura, M. (1999) *Nat. Struct. Biol.* **6,** 819–824
45. Berman, H. M., Westbrook, J., Feng, Z., Gilliland, G., Bhat, T. N., Weissig, H., Shindyalov, I., and Bourne, P. E. (2000) *Nucleic Acids Res.* **28,** 235–242
46. Tereshko, V., Teplova, M., Brunzelle, J., Watterson, D. M., and Egli, M. (2001) *Nat. Struct. Biol.* **8,** 899–907
47. Vakser, I. A. (1995) *Protein Eng.* **8,** 371–377
48. Fontes, M. R. M., The, T., Jans, D., Brinkworth, R. I., and Kobe, B. (2003) *J. Biol. Chem.* **278,** 27981–27987
49. Chakrabarti, P., and Janin, J. (2002) *Proteins* **47,** 334–343
50. Koradi, R., Billeter, M., and Wüthrich, K. (1996) *J. Mol. Graphics* **14,** 51–55
51. Urao, T., Katagiri, T., Mizoguchi, T., Yamaguchi-Shinozaki, K., Hayashida, N., and Shinozaki, K. (1994) *Mol. Gen. Genet.* **244,** 331–340
52. Sheen, J. (1996) *Science* **274,** 1900–1902
53. Zhao, Y., Pokutta, S., Maurer, P., Lindt, M., Franklin, R. M., and Kappes, B. (1994) *Biochemistry* **33,** 3714–3721
54. Weljie, A. M., Clarke, T. E., Juffer, A. H., Harmon, A. C., and Vogel, H. J. (2000) *Proteins* **39,** 343–357
55. DasGupta, M. (1994) *Plant Physiol.* **104,** 961–969
56. Chaudhuri, S., Seal, A., and DasGupta, M. (1999) *Plant Physiol.* **120,** 859–866
57. Chehab, E. W., Patharkar, O. R., Hegeman, A. D., Taybi, T., and Cushman, J. C. (2004) *Plant Physiol.* **135,** 1–17
58. Drykova, D., Cenklova, V., Sulimenko, V., Volc, J., Draber, P., and Binarova, P. (2003) *Plant Cell* **15,** 465–480
59. Gorlich, D., Kostka, S., Kraft, R., Dingwall, C., Laskey, R. A., Hartmann, E., and Prehn, S. (1995) *Curr. Biol.* **5,** 383–392
60. Imamoto, N., Shimamoto, T., Takao, T., Tachibana, T., Kose, S., Matsubae, M., Sekimoto, T., Shimonishi, Y., and Yoneda, Y. (1995) *EMBO J.* **14,** 3617–3626
61. Jiang, C., Shoji, K., Matsuki, R., Baba, A., Inagaki, N., Bani, H., Iwasakii, T., Imamoto, N., Yoneda, Y., Deng, X., and Yamamoto, N. (2001) *J. Biol. Chem.* **276,** 9322–9329
62. Kurokawa, H., Osawa, M., Kurihara, H., Katayama, N., Tokumitsu, H., Swindells, M. B., Kainosho, M., and Ikura, M. (2001) *J. Mol. Biol.* **312,** 59–68
63. Vetter, S. W., and Leclerc, E. (2003) *Eur. J. Biochem.* **270,** 404–414
64. Goldberg, J., Nairn, A. C., and Kuriyan, J. (1996) *Cell* **84,** 875–887
65. Velentza, A. V., Schumacher, A. M., Weiss, C., Egli, M., and Watterson, M. (2001) *J. Biol. Chem.* **276,** 38956–38965
66. Weljie, A. M., and Vogel, H. J. (2004) *J. Biol. Chem.* **279,** 35494–35502
67. Ofran, Y., and Rost, B. (2003) *J. Mol. Biol.* **325,** 377–387
68. Pazos, F., and Valencia, A. (2002) *Proteins* **47,** 219–227
69. Vandromme, M., Gauthier-Rouviere, C., Lamb, N., and Fernandez, A. (1996) *Trends Biochem. Sci.* **21,** 59–64
70. Jans, D. A. (1995) *Biochem. J.* **311,** 705–716

[6] A. Raichaudhuri, S. Chaudhuri, and M. DasGupta, unpublished observations.

Domain Analysis of a Groundnut Calcium-dependent Protein Kinase: NUCLEAR LOCALIZATION SEQUENCE IN THE JUNCTION DOMAIN IS COUPLED WITH NONCONSENSUS CALCIUM BINDING DOMAINS

Ayan Raichaudhuri, Rajasri Bhattacharyya, Shubho Chaudhuri, Pinak Chakrabarti and Maitrayee DasGupta

J. Biol. Chem. 2006, 281:10399-10409.
doi: 10.1074/jbc.M511001200 originally published online February 7, 2006
